Halloysite nanotubes filled with MgO for paper reinforcement and deacidification

Lorenzo Lisuzzo[a], Giuseppe Cavallaro[a,b,*], Stefana Milioto[a,b], Giuseppe Lazzara[a,b]

[a]Dipartimento di Fisica e Chimica, Università degli Studi di Palermo, Viale delle Scienze, pad. 17, 90128 Palermo, Italy. giuseppe.cavallaro@unipa.it

[b]Consorzio Interuniversitario Nazionale per la Scienza e Tecnologia dei Materiali, INSTM, Via G. Giusti, 9, I-50121 Firenze, Italy

Abstract

A novel material for the deacidification and protection of paper has been designed by using MgO filled halloysite nanotubes (Hal). The ability of MgO loaded nanotubes to control the acidic conditions was evaluated by pH measurements in aqueous solvent. Afterwards, paper was impregnated into hydroxypropyl cellulose dispersions containing the consolidating material. A simulation of strong acidic conditions allowed us to evaluate the deacidification effect of the composite material on the samples. In particular, the paper reaches a pH of 7.7 after 1 hour exposition to HNO_3 vapors when MgO-Hal nanoparticles are added to the impregnation mixture at a concentration of 10 wt % and it remains still neutral after 12 hours. Dynamic mechanical analysis showed that the tensile strength of the consolidated paper is improved, since the stress at breaking increase of ca. 8% for the samples treated with MgO-Hal compared to the untreated paper. Due to the presence of halloysite loaded with the alkaline reservoir, the acidic degradation of cellulose is neutralized as suggested by the stored energy which is similar to the pristine paper without any chemical attack. Therefore, the mechanical performances of the paper are preserved during the aging together with its macroscopic aspect, as suggested by colorimetric analysis. The proposed consolidation protocol represents a further step for the self-healing and long-term protection of cellulose based artworks.

Keywords: Halloysite nanotubes, cellulose, hydroxypropyl cellulose, DMA, paper consolidation, deacidification

1. Introduction

Paper is one of the most widespread material and, from the ancient times, it represents the most powerful tool that the mankind employed to transfer documents and to transmit knowledge to the future generations. The conservation of this treasure, which belongs to the common Cultural Heritage, is a societal issue and a technical challenge for restorers, librarians, and scientists.

Paper is made of cellulose, which is a linear homopolymer of (1-4)-linked β-D-glucopyranose units joined to create a highly ordered structure through intra and intermolecular hydrogen bonds (Oh et al., 2005). Several factors are responsible for the paper deterioration and, among them, atmospheric conditions (e.g. humidity, light, pollution), chemical reactions and biological activity play a major role (Poggi et al., 2016; Dresler et al., 2017; Girardi et al., 2017). The growth of fungi, bacteria or molds can lead to the degradation of paper due to the presence of cellulolytic enzymes and to the formation of spots that can deeply alter the aspect of manuscripts and historical documents, besides representing also a pathogenic and harmful risk to the human health (Flint et al., 2012; Brown et al., 2017). Hence, the biological attack has been fought by many different routes (Saladino et al., 2020). Literature reports the use of essential oils from aromatic or medicinal plants (thymol, cinnamon, etc.) with antimicrobial or antifungal activity, the integration of ionic liquids (ILs) components for the reinforcement against fungal infestations and the functionalization of nanocellulose for paper preservation and consolidation (Jiang et al., 2018; Schmitz et al., 2019; Bergamonti et al., 2020; Campanella et al., 2021). Nevertheless, the most diffused approaches exploit inorganic materials based on silver nanoparticles and metal oxides (e.g. zinc oxides or titanium dioxides), which possess a broad-spectrum antimicrobial activity and whose antimycotic properties are seldom investigated (Afsharpour et al., 2011; Afsharpour and Imani, 2017; Bergamonti et al., 2020; Motelica et al., 2020). Besides the biological issues, many efforts are also required to deal with the chemical reactions that occur within the paper (He et al., 2019). In particular, it has been found that the oxidation and acidic hydrolysis represents the main cause to the depolymerization and deterioration of cellulose-based artworks (Franceschi et al., 2001; Bogaard et al., 2005). The acidic-catalyzed mechanism is due to the adsorption of atmospheric pollutants and to the acidic additives, which are introduced during the papermaking and pulping processes (Area and Cheradame, 2011; Jiang et al., 2018). These species can act as catalysts of one of the most critical cause of paper degradation (Isca et al., 2019). As a consequence of the acidic hydrolysis, the breaking of glycosidic bonds occurs inside the fibers and it is responsible for the loss of mechanical performance of the paper (Marini et al., 2012). In addition, other acidic species are produced as oxidative products and they further play a role in increasing the degradation extent. Therefore, this mechanism is described as “auto-catalytic acidic hydrolysis” and it has detrimental effects on paper strength (Giorgi et al., 2002). As a result, the deacidification of

cellulose-based documents has become the most urgent and compelling challenge, and many different techniques have been designed in order to stop the acids formation. Magnesium and calcium hydroxides have been widely investigated for applications in this field, since they can act as an alkaline reservoir which can neutralize the creation of acidic species and can stop the hydrolysis reactions (Lienardy and Damme, 1990; M. and Bogaard John, 2009). It is worth to note that the dimensions of these particles allow for their penetration within the cellulosic matrix driving to the full impregnation of the paper texture (Poggi et al., 2014). Recently, the scientists provided more advanced tools for the consolidation and deacidification of lignocellulosic artwoks by using natural resources (Broda, 2020), organosilicons (Broda et al., 2020) and nanostructured materials (Giorgi et al., 2005; Jiang et al., 2020; Sadjadi, 2020). Among the nanomaterials, halloysite nanotubes (Hal) hold a certain importance. Halloysite is a natural occurring aluminosilicate that can be extracted from different deposits in several regions (Lazzara et al., 2018). Depending on the localization, the dimensions of the hollow tubular nanoclay may vary from 50 to 100 nm for the external diameter, from 15 to 50 nm for the inner diameter and from 0.2 to 3 μm for the length (Lvov et al., 2008; Pasbakhsh et al., 2013). Structurally, the nanotubes are composed by a Si-O-Si tetrahedral sheet that is overlapped to an octahedral gibbsite-like array of aluminols (Zhao et al., 2015; Sadjadi et al., 2017). Due to the different chemistry, the internal and the external surfaces of halloysite are oppositely charged, being the Si-based outer surface is negative and the Al-based inner surface is positive in a wide pH range (Abdullayev et al., 2012; Bugatti et al., 2017; Y. Zhang et al., 2019). Halloysite received a great interest from the scientific community due to the most diverse application fields where it can be exploited and to its biocompatibility and low toxicity (Fakhrullina et al., 2015; Kryuchkova et al., 2016; Vinokurov et al., 2017; Ariga et al., 2018; García-Vázquez et al., 2020; Zhao et al., 2020; Rozhina et al., 2021). For instance, literature reports that the addition of nanoclays to a polymeric matrix causes the improvement of both thermal and mechanical properties of the resulting composite bioplastics when the nanofillers are homogeneously dispersed (Gorrasi et al., 2014; Makaremi et al., 2015; Spepi et al., 2016; Nunes et al., 2018; Barra et al., 2020; Dang et al., 2020; Yang et al., 2020). This effect is crucial, among others, for the treatment of cellulose based materials (Bertolino et al., 2020). Besides, the unique morphology of this class of inorganic nanotubes allows for the loading of their inner volume with chemically and biologically active species (Dzamukova et al., 2015; Gorrasi, 2015; Yang et al., 2016; Yamina et al., 2018; Cheng et al., 2020). The encapsulation of molecules within the lumen of halloysite predicts its most interesting features, since it can act as nanocontainer and delivery system for several compounds regardless of their specific hydrophilic or hydrophobic properties (Lvov et al., 2016; Dramou et al., 2018; H. Zhang et al., 2019; Liu et al., 2020). As a consequence, halloysite nanotubes have been used for the design of

nanostructured materials to be employed in catalysis, environmental science, cosmetics and health technology, food packaging and for the protection of cultural heritage (e.g. waterlogged archeological woods, marble surfaces and paper) (Viseras et al., 2009; Owoseni et al., 2014; Liu et al., 2016; von Klitzing et al., 2016; Hermawan et al., 2018; Zhao et al., 2018; Cavallaro et al., 2020b, 2020c; Fizir et al., 2020; Lisuzzo et al., 2021). Different protocols were developed for the conservation of manuscripts and ancient documents, ranging from the use of halloysite dispersions in cellulose based biopolymers to nanotubes filling with antiacids for the long-term active protection of paper (Cavallaro et al., 2014, 2017).

In this work we moved forward by reporting an innovative strategy for the loading of halloysite with MgO that can act as alkaline reservoir for the treatment and deacidification of paper. It should be noted that the solubility of magnesium oxides or hydroxides is very low in aqueous media. Moreover, magnesium hydroxide nanoparticles appear with a stronger reactivity and fast carbonatation (Poggi et al., 2010). The proposed protocol succeeded in overcoming these issues. Indeed, the electrostatic interactions between the nanotubes and the antiacid precursors were exploited during the loading step and the alkaline payload was directly created inside the nanoclays.

Once the protecting nanomaterial was prepared, the paper-based samples were treated by the impregnation method in hydroxypropyl cellulose, which is an ether of cellulose, and it demonstrated to be efficient in controlling the pH conditions even upon a strong acidic simulation (Okahashi et al., 2021). Furthermore, the mechanical properties of paper were improved after the consolidation as a consequence of the nanofillers efficiency and due to their alkaline activity, which is responsible for the neutralization of the acidic hydrolysis and degradation. Hence, the proposed protocol represents an innovative tool for the design of antiacid nanotubular fillers that can be successfully employed for the time-extended protection of cellulose based artworks.

2. Materials and Methods

2.1. Materials

Ethylenediaminetetraacetic acid (EDTA - $C_{10}H_{16}N_2O_8$, anhydrous), halloysite (specific surface area of 65 m^2 g^{-1} and specific gravity of 2.53 g cm^{-3}), Magnesium chloride hexahydrate ($MgCl_2 \cdot 6H_2O$, 99.0-102.0%), NH_4Cl/NH_3 buffer solution, Hydroxypropyl Cellulose (HPC, M_w ~80,000, M_n ~10,000) and HNO_3 (nitric acid, 60%) were purchased from Sigma-Aldrich and used without any further purification. The paper sample (thickness 0.15 mm, 73 g m^{-2} and water capillary raise >178 mmh^{-1}) was from Albet®.

2.2. Loading of MgO within halloysite

In order to load halloysite with MgO we firstly prepared an aqueous solution of $MgCl_2$ with a stoichiometric amount of EDTA in buffered alkaline conditions, namely pH = 8 in NH_4Cl/NH_3. The accurate choice of pH can be explained by considering both the charge of Hal, whose inner surface is still positive, and the charge of EDTA, which is in its monoprotonated state HY^{3-} (Liu et al., 2004). After the interaction with Mg^{2+}, the negative $MgEDTA^-$ species are formed and their interaction with the inner lumen of the nanoclays is optimized. Hence, pristine halloysite (2 wt%) was added and the suspension was sonicated for 10 min. To improve the loading efficiency, the system was kept under vacuum for 1 hour and then it was brought back to the atmospheric pressure and stirred for additional 30 minutes. The vacuum in/out cycles were repeated 3 times, according to literature (Lisuzzo et al., 2019b). Afterwards, the $MgEDTA^-$ loaded nanotubes were separated from the aqueous phase by centrifugation, washed three times to remove any excess and dried overnight at 50 °C. A calcination step was also conducted at 700 °C to induce the thermal degradation of the organic moieties, finally resulting in the formation of MgO species within halloysite nanotubes (Figure 1).

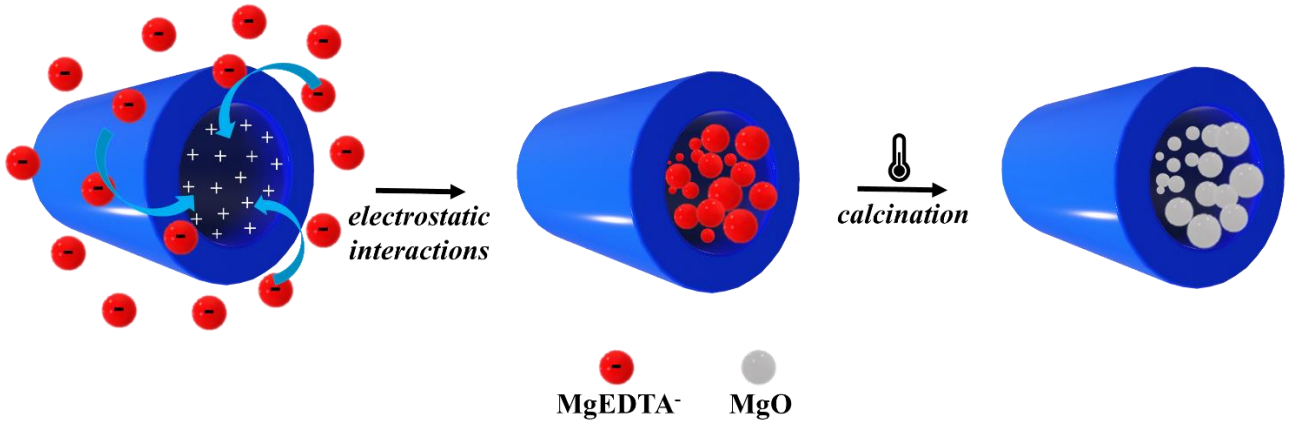

Figure 1. Scheme of the preparation procedure of MgO loaded halloysite.

158 *2.3. Impregnation of paper for protection*

159 For the treatment of paper an aqueous solution of HPC at 2 wt % was prepared. Then, it was divided
160 in different aliquots and a certain amount of MgO-Hal (from 0 to 20 wt%) was added to the polymer
161 solutions and kept under stirring overnight at 25 °C. The paper was cut in rectangular samples (40
162 mm × 5 mm) that were deeply immersed into the aqueous HPC/MgO-Hal dispersions for 24 h at 20
163 °C. After the impregnation, the treated samples were dried out at 35 °C. The amount of protecting
164 material for each treated sample was evaluated by gravimetric analysis (±0.00001 g). The paper
165 samples were re-equilibrated with air for 3 days before characterization.

166 *2.4. Paper aging under acidic conditions*

167 The samples of both treated and untreated paper were exposed to acidic vapours, which mime aging
168 conditions. With this aim, they were placed in a closed desiccator with a solution of HNO_3 30 wt %
169 to create an acid saturated atmosphere. After the exposition to acidic vapours for variable time
170 intervals (up to 12 hours), the paper samples were re-equilibrated with air for 3 days before further
171 analysis.

172 *2.5 Characterization methods*

173 A Zetasizer NANO-ZS (Malvern Instruments) was used to conduct ζ-potential experiments, which
174 were carried out at 25 °C. Thermogravimetric analysis (TGA) was performed by using the Q5000 IR
175 (TA Instruments) apparatus under N_2 flow, which was 25 cm^3 min^{-1} for the sample and 10 cm^3 min^{-1}
176 for the balance, respectively. The samples were heated from room temperature up to 800 °C with a
177 scanning rate of 20 °C min^{-1}. The instrumental calibration was conducted on the basis of the Curie
178 temperatures of standards (nickel, cobalt, and their alloys) (Blanco et al., 2014, 2017). The loading
179 amounts within the cavity of halloysite nanotubes were calculated through the rule of mixtures as
180 reported in literature (Lisuzzo et al., 2019b). The pH measurements were carried out by means of a
181 PCD650 pH meter (Eutech Instruments) which was immersed into the aqueous dispersions of MgO,
182 halloysite and MgO loaded halloysite under stirring conditions. The pH values of the paper samples,
183 instead, was measured at certain times intervals through a HI 1413B/50 portable pH meter with a flat-
184 tip electrode (Hanna Instruments) after rinsing its tip with a droplet of water. Dynamic Mechanical
185 Analysis (DMA) was conducted by a DMA Q800 apparatus (TA Instruments) allowed us to evaluate
186 the tensile properties of paper. Rectangular samples were studied under a stress ramp of 1 MPa min^{-1}
187 at 25.0 ± 0.5 °C. We determined the mechanical performances in terms of stress at breaking (σ_r) and
188 energy stored at the sample fracture. The latter was calculated by integrating the stress vs strain
189 curves. An ESEM FEI QUANTA 200F electronic microscope was used to investigate the morphology

of the materials. To avoid charging under the electron beam, each sample was coated with Au in argon by means of an Edwards Sputter Coater S150A. The measurements were conducted in high vacuum mode (<6 x 10^{-4} Pa) for simultaneous secondary electrons; the energy of the beam was 25 kV and the working distance was 10 mm. Colorimetric analysis was performed using a NH300 Colorimeter (3NH Shanghai Co., Ltd.) which was calibrated using black and white plates. CQCS3 Software was used for the data collection of L* (lightness), a* (red−green), and b* (yellow−blue) parameters. The total color difference (ΔE) between samples was calculated as reported in literature by considering three different points (Yousefi et al., 2020).

3. Results and Discussion

3.1. Characterization of MgO-Hal aqueous dispersions

The choice to load halloysite with $MgEDTA^-$ for the preparation of MgO-Hal nanoparticles upon calcination, instead of using MgO or $Mg(OH)_2$ in the preparation protocol is strategic. Indeed, the water solubility of magnesium oxide or hydroxide is very low and, as a consequence, the direct encapsulation of these alkaline species within the cavity of the nanotubes shows several issues and it was not successful. Hence, we started by using $MgCl_2$ and EDTA in aqueous solution at pH = 8 to optimize the yield of the monoprotonated state of the organic counterpart to give $MgEDTA^-$ after interaction with the Mg^{2+} cations. It is worth to note that, in these conditions, the inner surface of halloysite is still positive so that the electrostatic interactions between the oppositely charged components play a crucial role (Cavallaro et al., 2020a).

With this in mind, ζ potential measurements were carried out to evaluate the interactions between halloysite nanotubes and the anionic complexes at the same pH conditions. Table 1 reports the values for pristine nanotubes and $MgEDTA^-$ loaded nanotubes.

Table 1. ζ potential values for pure and $MgEDTA^-$ loaded halloysite nanotubes at pH = 8.

Sample	ζ potential (mV)
Hal	-24.9 ± 0.3
$MgEDTA^-$ loaded Hal	-45.1 ± 0.9

It can be clearly observed that, after the interactions between the anionic species and the nanoclay, the ζ potential shifts towards more negative values. This effect can be related to the effective encapsulation of $MgEDTA^-$, which neutralizes the positive inner charges of the alumina surface within the lumen leading to a higher net negative charge for the system. Similar results are reported

in literature for sodium alkanoates and sodium dodecyl sulfates (Lisuzzo et al., 2019a). In order to evaluate the loading efficiency we performed thermogravimetric analysis. Thermogravimetric curves for pure Hal, pure $MgEDTA^-$ and $MgEDTA^-$ loaded Hal are reported in Figure 2.

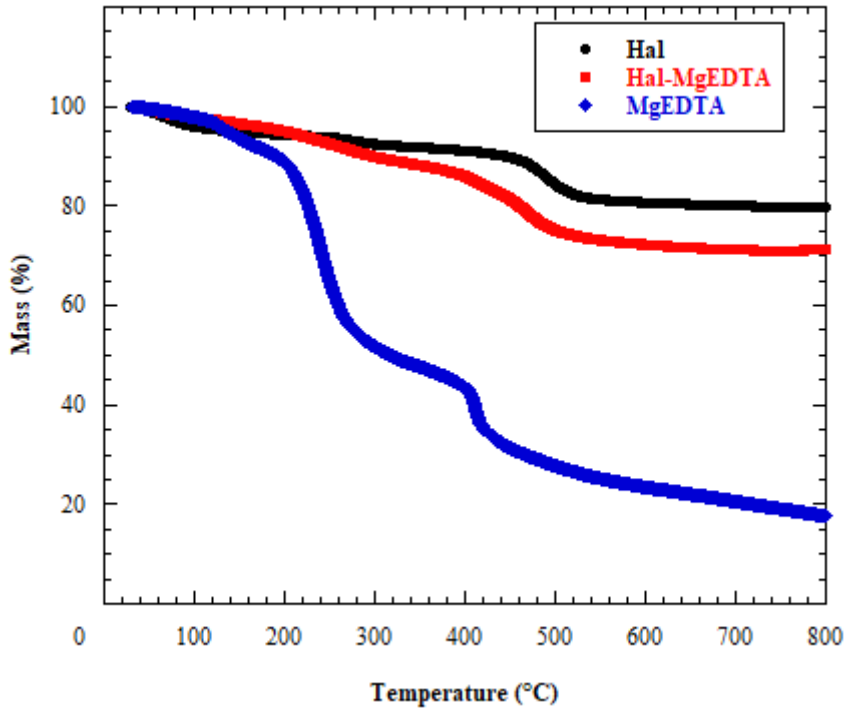

Figure 2. Thermogravimetric curves of pristine Hal, MgEDTA and $MgEDTA^-$ loaded Hal.

The raw nanoclays showed a mass loss between 50 °C and 150 °C, which is related to the moisture content and desorption of water molecules (Blanco and Siracusa, 2021), whereas the typical dehydroxylation of structural Al–OH groups can be observed between 450–500 °C, as confirmed in literature (Duce et al., 2015). Similarly, the first weight loss in the curve of MgEDTA corresponds to the water content. Most importantly, the two principal stages of thermal degradation in the 200-450 °C range can be ascribed to the decomposition of the ligand and to the removal of $–COO^–$ and $–N(C_yH_z)_x$ moieties (Tarasov et al., 2011). It is clear that the degradation extent of the organic counterpart is higher, resulting in a lower residual matter at 800 °C for pure MgEDTA. Similar observations can be done for the MgEDTA loaded halloysite, whose residual mass is lower compared to pristine halloysite due to the presence of the organic payload.

By comparing the thermograms of the three samples and using the rule of mixtures, we estimated the amount of MgO encapsulated within halloysite. On this basis, it was calculated that the MgO loading is 2.2 ± 0.1 wt % which corresponds to 1.6 ± 0.1 v/v %.

Afterwards, aimed at assessing the antiacid properties of the MgO loaded halloysite nanotubes, the pH values of aqueous dispersions were measured at pre-established intervals of time to investigate the release kinetics of the alkaline reservoir (Figure 3).

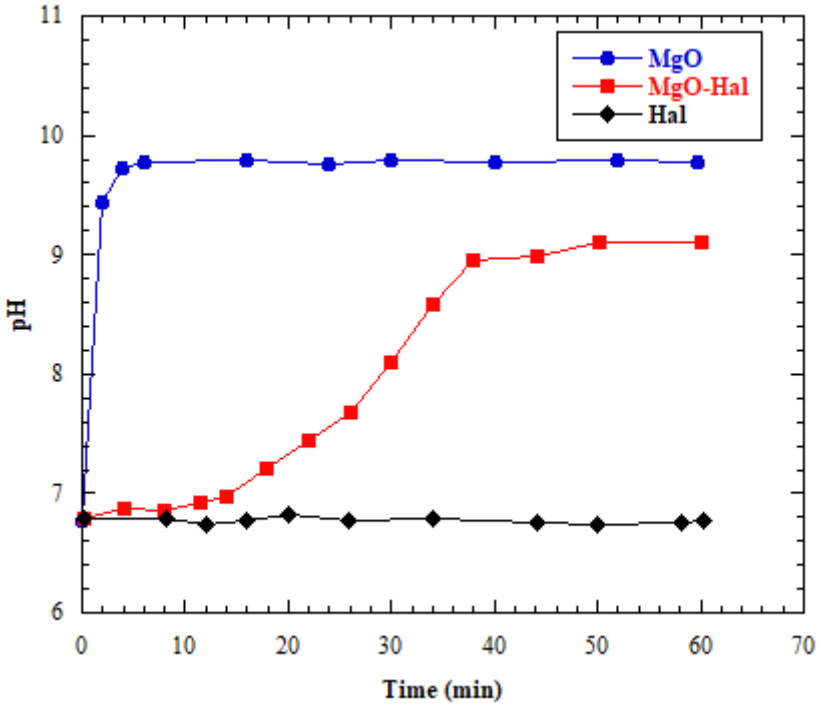

Figure 3. pH values of Hal, MgO and MgO-Hal aqueous dispersions as a function of time.

It is clear that pristine nanotubes do not play a role in affecting the acidic conditions of the aqueous dispersion, being the trend constant at pH ≈ 6.8 even after 60 minutes. Conversely, a blank experiment reporting the kinetics for pure MgO revealed a quick dissolution of the oxide. The presence of MgO species in water is responsible for a sudden increase of the pH due to their strong alkaline properties. Indeed, the pH is ca. 9.5 after only 2 minutes and it reaches a maximum of 9.8 after 6 minutes, then remaining constant in the whole range of time. As concerns MgO-Hal, it is noteworthy that the variation of pH is slowed down. In particular, the curve reported in Figure 3 shows a sustained increase with a maximum value of pH ≈ 9 reached after 40 minutes, which is thereafter maintained. These findings can be most likely related to the effective encapsulation of the alkaline species within the cavity of the hollow nanotubular clay. Before being fully available in the aqueous medium, MgO species must diffuse through the lumen and this particular mechanism has been reported to deeply influence the release kinetics of active molecules, such as drugs, due to the diffusion path (Lisuzzo et al., 2020b).

3.2 Effect of MgO-Hal on paper treatment

In order to evaluate the efficiency of the consolidation protocol, the amount of protecting material for each paper sample was estimated by gravimetric analysis after the treatment. Namely, the mass of the samples was measured after the impregnation in the aqueous solution of HPC with different amounts of MgO-Hal. The values are reported in Figure 4. Herein, the treatment efficiency represents the content of the protecting material (HPC + MgO-Hal) in the consolidated paper samples, whilst MgO-Hal is the percentage of the loaded halloysite nanotubes added to the HPC solution.

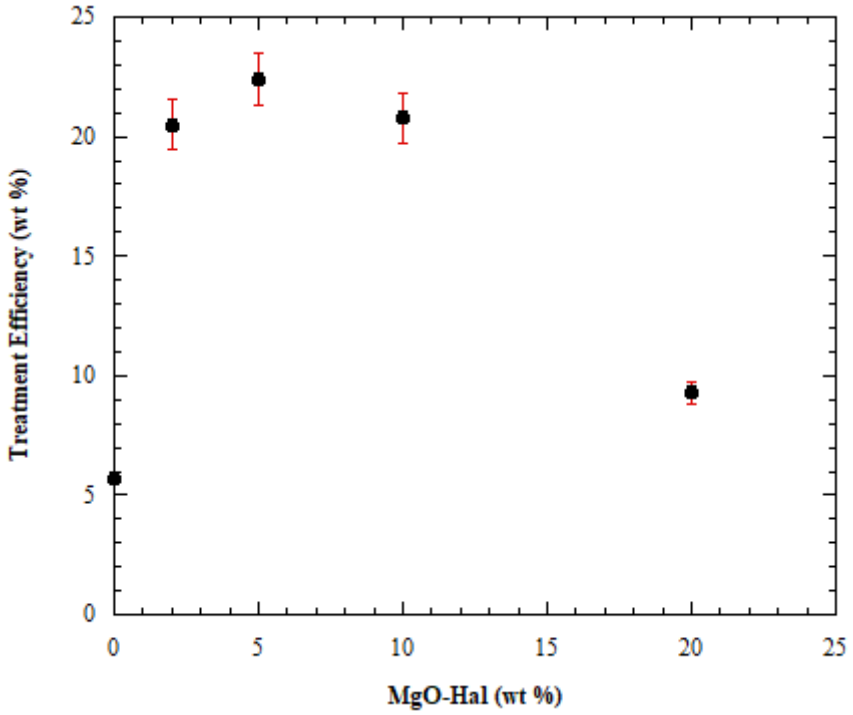

Figure 4. Treatment efficiency as a function of the MgO-Hal concentration in the consolidating mixture.

It is clear that the concentration of the overall protecting material increases when MgO-Hal are added during the treatment protocol. Indeed, values are reported to be 5 wt% when only HPC is employed and they soared up to 20-23 wt% after the addition of the inorganic counterparts from 2 to 10 wt%. Conversely, when the amount of MgO-Hal in the impregnation mixture is 20 wt % the concentration of the treating material decreases to ca. 9 wt %. This effect can be most likely related to the aggregation of nanotubes and to the formation of clusters, which cannot penetrate the cellulosic matrix of paper and cannot act as functional fillers.

To corroborate this hypothesis, the morphology of the paper after the treatment was investigated by Scanning Electron Microscopy. We observed that the protecting material is homogeneously dispersed within the cellulosic matrix when the concentration of MgO-Hal is 10 wt% and no clusters can be

seen (Figure 5A). In this case, the surface appears to be smooth and the different nanoparticles can be separately distinguished in the higher magnification image (Figure 5B). Conversely, the paper sample treated with 20 wt% MgO-Hal presents a not uniform and rough surface (Figure 5C) and the dispersion of the antiacids loaded nanotubes within the texture of paper is not homogeneous, but they agglomerate into clusters of larger dimensions (Figure 5D).

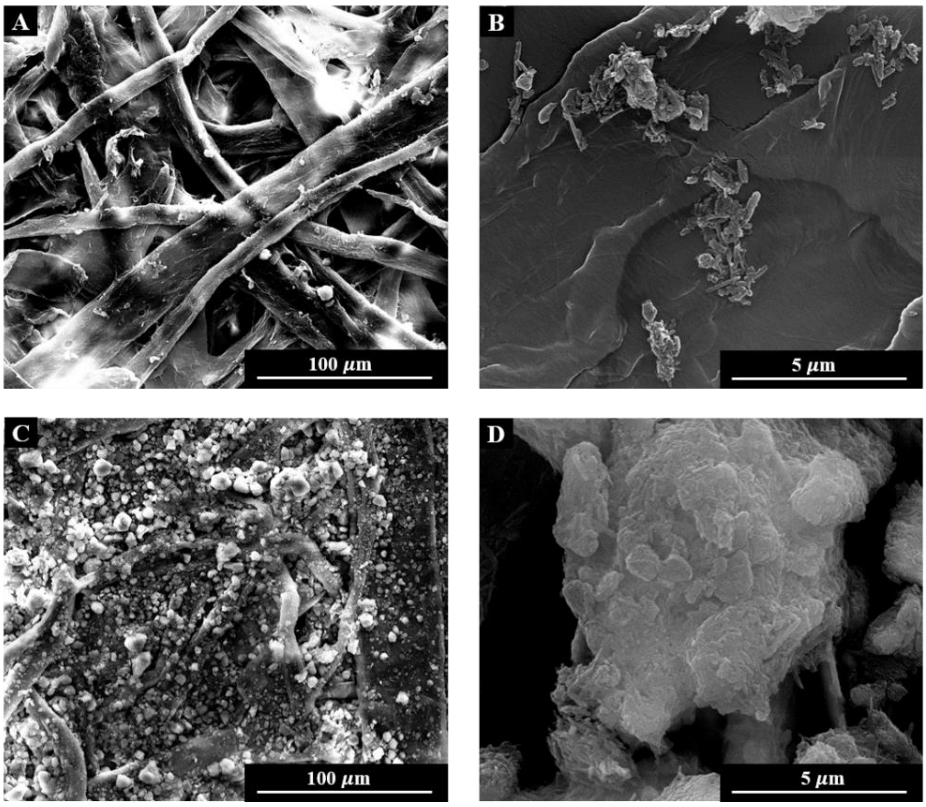

Figure 5. SEM micrographs for paper treated with MgO-Hal 10 wt% (A,B) and MgO-Hal 20 wt% (C,D) in HPC mixtures.

The antiacid properties of the composite material used for the treatment of the paper samples were evaluated by pH measurements as functions of both time and concentration of the alkaline reservoir after being exposed to acidic vapours (Figure 6).

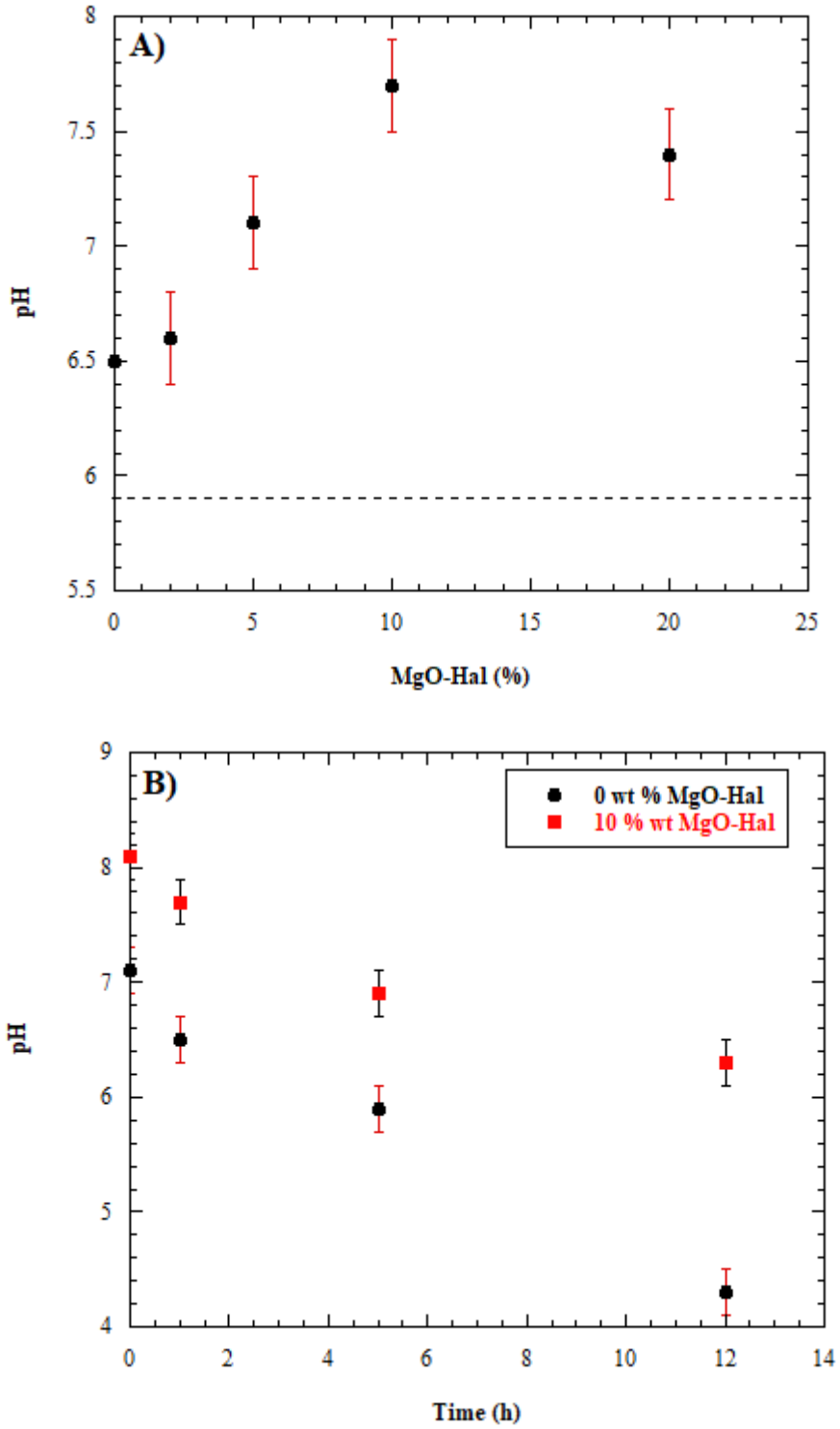

Figure 6. (A) pH values of treated paper samples as a function of MgO-Hal concentration after 1 hour of exposure time to HNO_3 vapours. (B) pH values as a function of exposure time to HNO_3 vapours for paper samples treated with 0 and 10 % wt MgO-Hal.

As it can be clearly observed in Figure 6A, the pH increases as the concentration of the MgO-Hal particles increases. The measured pH value for the pure hydroxypropyl cellulose treated paper is 6.5 after 1 hour exposition to nitric acid vapours, and it reaches a maximum of 7.7 when halloysite loaded with the alkaline species is added to the impregnation mixture at a concentration of 10 wt %. It should be noted that the pH for the untreated sample is the lowest after 1 hour of aging, namely 5.9 (dotted line in Figure 6a). As long as the concentration of the antiacid fillers is 20 wt %, instead, the pH shows a slight decrease to 7.4 in the same range of time. In light of these results, it is possible to state that the treatment with pure HPC is responsible for a certain effect on the pH of aged paper but the presence of the alkaline reservoir within the lumen of halloysite plays a major role. As evidenced, the neutralizing effect towards the acidic aging increases with the MgO-Hal content in the treating material up to a certain extent. Then, the smaller effect observed for the highest concentration of antiacid particles is in agreement with the previous results (treatment efficiency and SEM analysis). Due to the formation of large aggregates, the MgO loaded halloysite cannot penetrate the matrix of paper, with a lower efficiency in controlling its pH after aging under acidic conditions.

In Figure 6B we reported the pH trends as function of time for paper samples treated with HPC (0 wt % MgO-Hal) and HPC/MgO-Hal 10 wt %. Here again, we took into account the duration time of exposition to the HNO_3 vapors. The starting values (exposure time = 0 h) are 7.1 and 8.1 for 0 wt % and 10 wt % of MgO-Hal, respectively. Then, the pH decreased to 4.3 for the former and to 6.3 for the latter after 12 hours. Although an overall decrease can be observed in both cases, it is noteworthy that the paper sample treated with the antiacid nanofillers remains still neutral. Conversely, the pH turns to highly acidic values after the treatment without alkaline payload. This effect can be related to the sustained MgO release from the cavity of halloysite. It should be considered that the environmental conditions used for the aging simulation are strongly acidic compared to the conventional conservation places. Therefore, the obtained results appear to be very promising.

Furthermore, the mechanical performances of the treated paper were investigated in order to evaluate the effects of both the consolidation protocol and of the acidic aging. Some examples of stress vs. strain curves are shown in Figure 7.

Table 2 reports the stress at breaking (σ_r) of the samples and its variation compared to untreated paper ($\Delta\sigma_r$) after the treatment with the MgO-Hal composite at different concentrations. The 0 wt % MgO-Hal sample represents the treatment with pure hydroxypropyl cellulose. Curves in Figure 6 and values in Table 2 are referred to untreated and treated samples before acidic aging.

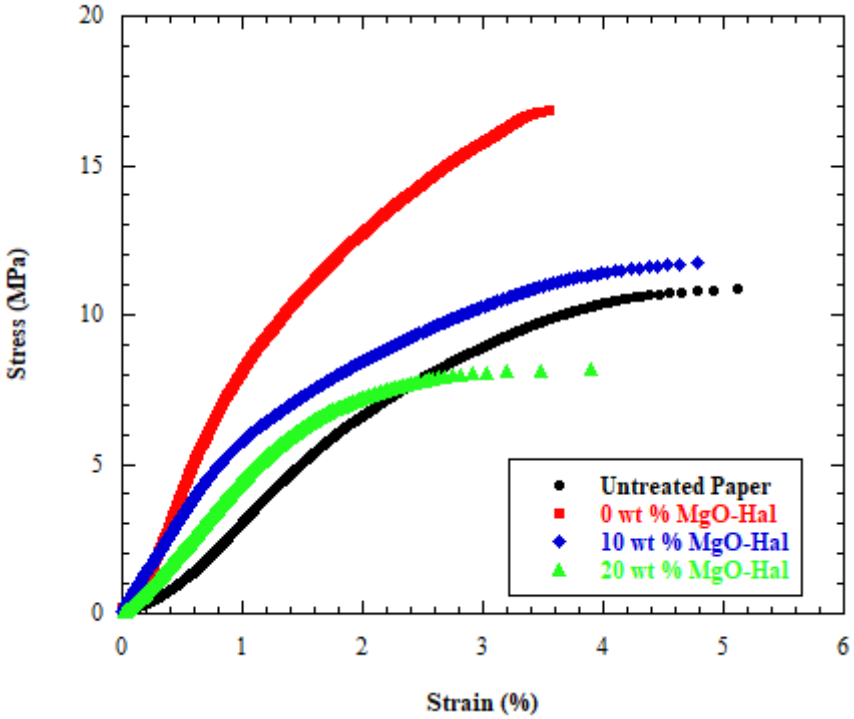

Figure 7. Stress vs. strain curves for untreated and treated paper samples before acidic aging.

Table 2. Stress at breaking values (σ_r) of untreated and treated samples before acidic aging. $\Delta\sigma_r$ represents the variation of the tensile strength after the treatment.

Sample	σ_r (MPa)[a]	$\Delta\sigma r$ (%)
Untreated Paper	10.8	
0 wt % MgO-Hal	16.8	55.5
2 wt % MgO-Hal	11.7	8.3
5 wt % MgO-Hal	11.6	7.4
10 wt % MgO-Hal	11.7	8.3
20 wt % MgO-Hal	8.2	-24.1

[a] The relative error is 2 %.

For what concerns the paper treated with HPC, the tensile strength increases up to 16.8 MPa, which means 55.5 % compared to the untreated sample. This reinforcement can be ascribed to the presence of the biopolymer, which is responsible for an improved connection between the fibers in the matrix of paper, thus providing mechanical resistance. Once the MgO-Hal particles are included in the HPC solution for the impregnation of paper, instead, there is a double effect. In particular, the measured values of stress at breaking increase of ca. 8% for the samples treated with 2, 5 and 10 wt % MgO-Hal compared to the untreated paper. Conversely, the tensile strength shows a strong decrease after

the treatment with 20 wt % of MgO loaded nanotubes, and namely the variation is -24.1% compared to the untreated paper.

These results can be most likely due to the different dispersion of the nanoclay within the paper as observed by SEM. Once halloysite is homogenously distributed, the adhesion between the clay and the polymeric matrix of paper is enhanced, thus being responsible for the overall improvement of the mechanical properties. On the opposite side, the tensile strength is reduced by the non-uniform dispersion of the antiacid loaded nanofillers when the concentration is too high. It is worth to note that these findings are in agreement with both the treatment efficiency, which is lower for the 20 wt % MgO-Hal treated sample, and with the effects on pH. The aggregation of the nanotubes and the formation of clusters play a role also in the worsening of the tensile properties of the resulting material. In addition, similar results were reported for other polymeric composites and bioplastics (Chivrac et al., 2010; Lisuzzo et al., 2020a).

At this point, we moved forwards by investigating the mechanical performances of the prepared samples after 12 h of aging procedure under HNO_3 vapours. To this purpose, the stored energy was calculated by integrating the stress vs strain curves. Figure 8 reports ΔSE (%) values, which are the variations of the stored energies up to the breaking induced by the acidic aging.

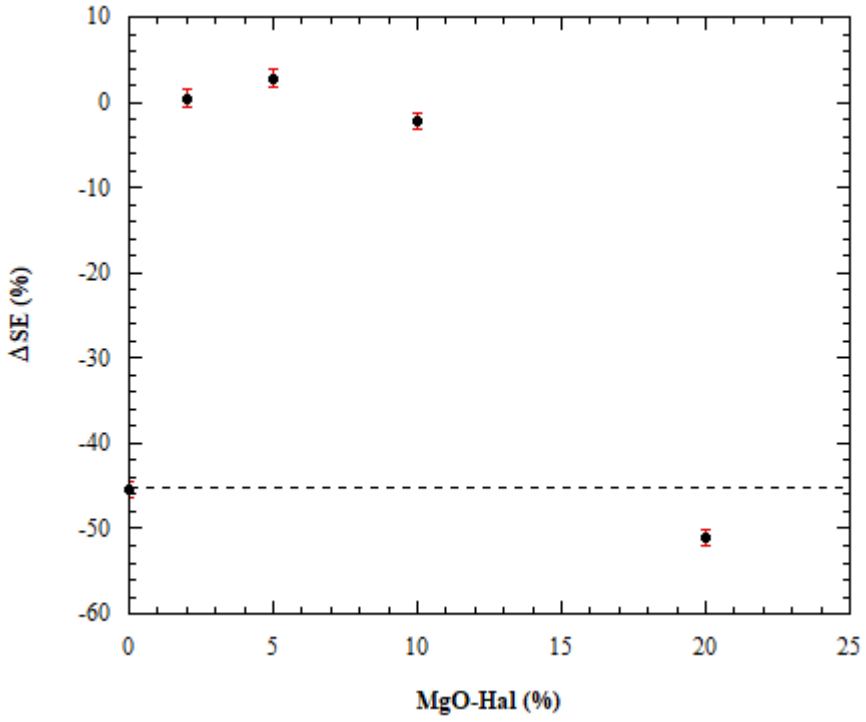

Figure 8. ΔSE values for treated samples as a function of the MgO-Hal concentration. Dotted line is the value for untreated paper.

Notwithstanding the improvement of the tensile strength, as suggested by the aforementioned increase of the stress at breaking point, the energy stored by the paper treated only with HPC (0 wt % MgO-

Hal) strongly decreases upon acidic aging. In particular, ΔSE is - 45.4% and it corresponds to the value measured for the untreated paper exposed to HNO_3 vapours (dotted line in Fig. 8). Hence, the mechanical performances of both the pristine paper and the HPC treated paper are worse after the aging simulation compared to pristine paper before the aging. Contrarily to them, the samples treated also with MgO-Hal show, after the acidic aging, values of stored energy similar to the pristine paper without chemical attack. In these cases, ΔSE values are included between +2.8 and -2.2 %. The different mechanical features can be explained by considering the antiacid properties of halloysite filled with an alkaline reservoir, which was able to minimize the loss of tensile performance. Indeed, MgO can be released over time and it neutralizes the acidic degradation due to the atmospheric conditions. As a consequence, the mechanical performances of the 2, 5 and 10 wt % MgO-Hal treated samples are similar to those of the pristine paper before acidic aging, and these systems are more efficient in strengthening the material keeping relatively high *SE* values even if they underwent a strong aging simulation. As expected, the paper treated with 20 wt % MgO-Hal undergoes a reduction of the stored energy that is -51.1%. Since the concentration of nanofiller is too high to penetrate the matrix of paper and to favourably interact with the polymeric chains, halloysite is not homogeneously dispersed and the low amount of nanotubes with an alkaline reservoir cannot neutralize the acidic attack. As a consequence, the mechanical performances resulted to be worsened. Similar findings are also reported in literature. For instance, the elongation at break and the stored energy of eco-compatible bioplastics can be improved by a small amount of clay nanotubes. Then, further nanofiller additions result in the worsening of the thermo-mechanical properties due to the peculiar morphological features of the composites. The homogenous distribution of inorganic fillers within the polymeric matrix can cause an enhancement of the thermal stability and mechanical stiffness. Conversely, the presence of a rough surface with clusters worsens the overall properties of the material ((Lisuzzo et al., 2020a).

Aimed at assessing the effects of the treatment on the paper samples and on their appearance, we perfomed colorimetric analysis and reported the colorimetric parameters in Table S1 (see Supplementary material).

In particular, it was found that the total color difference (ΔE) between the untreated and the treated paper is 0.095, thus meaning that the macroscopic aspect of the samples was not affected after the proposed protocol was carried out (Meng et al., 2014; Sharma et al., 2017). Moreover, the writing quality of the treated paper did not change (Figure 9).

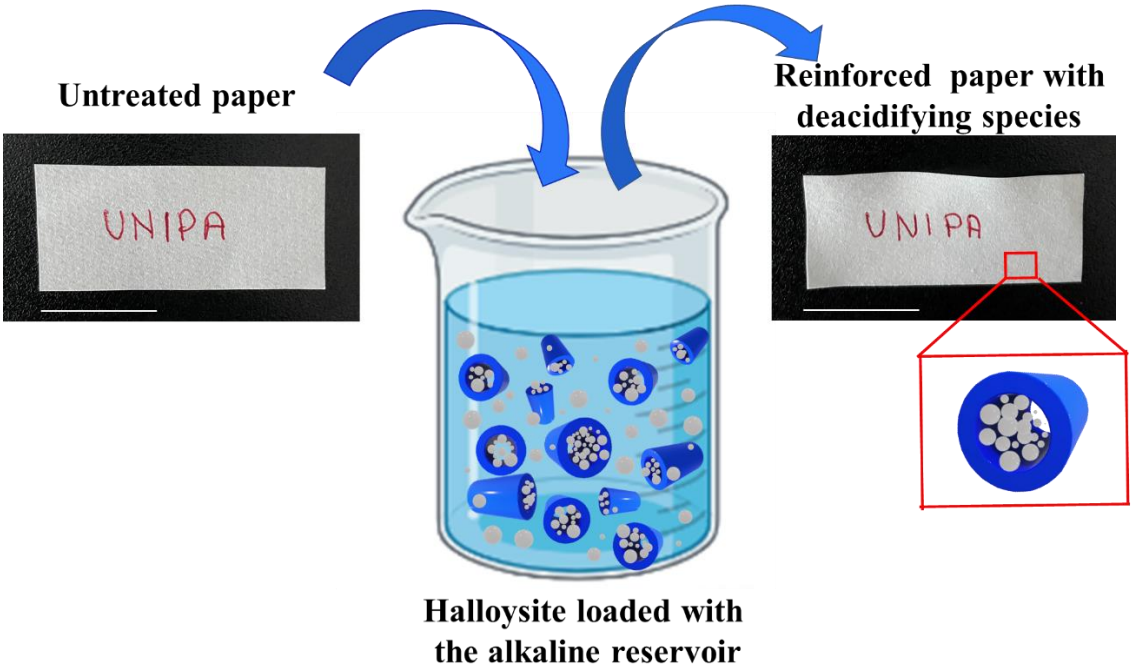

Figure 9. Optical photos of the paper before and after treatment with 10 wt % MgO-Hal in HPC. The scale bars are 2 cm. "UNIPA" was written with a ball pen.

4. Conclusions

In this work, we designed a novel protocol for the loading of halloysite nanotubes (Hal) with an alkaline reservoir that can be exploited for the treatment of cellulose-based paper.

Due to the low solubility of magnesium oxide, $MgCl_2$ and EDTA were employed for the preparation strategy. The formation of $MgEDTA^-$ complexes and their successful encapsulation within the inner cavity of halloysite were confirmed by ζ-potential measurements whereas thermogravimetric analysis allowed us to evaluate the effective loading of the nanoclays with MgO species. The antiacid properties of the payload were studied by pH measurements in order to have more precise insights about the sustained release of MgO from the lumen of the nanotubes.

Afterwards, paper samples were treated by the impregnation method in hydroxypropyl cellulose/MgO-Hal dispersions and the treatment efficiency was estimated. We carried out a simulation of strong acidic aging conditions by HNO_3 vapours and it was found that the consolidation protocol plays a crucial role in controlling the pH of the paper even after the acidic attack. In particular, the pH of the material increases with the amount of the MgO-Hal particles up to certain concentration, namely 10 wt %. Moreover, the paper sample treated with the antiacid nanofillers remains still neutral although the exposure for 12 hours to the acidic atmosphere.

Furthermore, the mechanical properties of the materials were investigated by Dynamic Mechanical Analysis in order to evaluate the effects of the consolidation protocol before and after the aging simulation. We found that the tensile properties of the paper resulted to be improved after the impregnation step in HPC and MgO-Hal. More interestingly, the presence of the antiacids loaded nanofillers neutralizes the HNO_3 vapors attack during the aging procedure, thus minimizing the loss of mechanical performances. The materials treated with a concentration of MgO-Hal up to 10 wt % resulted to be strengthened and they can undergo the strong acidic atmosphere but still showing tensile features similar to pristine paper before aging. Additional amounts of nanoparticles did not show better protection as the clay clustering prevented from a successful dispersion and impregnation efficacy of the paper sample as observed by SEM analysis. Besides, the colorimetric properties and the writing quality of the paper did not change after the treatment. To the light of these findings, the proposed protocol appears to be very promising for the tailored loading of halloysite nanotubes and for the successful protection and self-healing of cellulosic paper.

5. Acknowledgements: The authors acknowledge the University of Palermo for financial support.

6. References

Abdullayev, E., Joshi, A., Wei, W., Zhao, Y., Lvov, Y., 2012. Enlargement of Halloysite Clay Nanotube Lumen by Selective Etching of Aluminum Oxide. ACS Nano 6, 7216–7226. https://doi.org/10.1021/nn302328x

Afsharpour, M., Imani, S., 2017. Preventive protection of paper works by using nanocomposite coating of zinc oxide. J. Cult. Herit. 25, 142–148. https://doi.org/10.1016/j.culher.2016.12.007

Afsharpour, M., Rad, F.T., Malekian, H., 2011. New cellulosic titanium dioxide nanocomposite as a protective coating for preserving paper-art-works. J. Cult. Herit. 12, 380–383. https://doi.org/10.1016/j.culher.2011.03.001

Area, M.C., Cheradame, H., 2011. Paper aging and degradation: recent findings and research methods. BioResources 6, 5307–5337.

Ariga, K., Leong, D.T., Mori, T., 2018. Nanoarchitectonics for Hybrid and Related Materials for Bio-Oriented Applications. Adv. Funct. Mater. 28, 1702905. https://doi.org/10.1002/adfm.201702905

Barra, A., Alves, Z., Ferreira, N.M., Martins, M.A., Oliveira, H., Ferreira, L.P., Cruz, M.M., Carvalho, M. de D., Neumayer, S.M., Rodriguez, B.J., Nunes, C., Ferreira, P., 2020. Biocompatible chitosan-based composites with properties suitable for hyperthermia therapy. J Mater Chem B 8, 1256–1265. https://doi.org/10.1039/C9TB02067E

Bergamonti, L., Potenza, M., Haghighi Poshtiri, A., Lorenzi, A., Sanangelantoni, A.M., Lazzarini, L., Lottici, P.P., Graiff, C., 2020. Ag-functionalized nanocrystalline cellulose for paper preservation and strengthening. Carbohydr. Polym. 231, 115773. https://doi.org/10.1016/j.carbpol.2019.115773

Bertolino, V., Cavallaro, G., Milioto, S., Lazzara, G., 2020. Polysaccharides/Halloysite nanotubes for smart bionanocomposite materials. Carbohydr. Polym. 245, 116502–116513. https://doi.org/10.1016/j.carbpol.2020.116502

Blanco, I., Abate, L., Bottino, F.A., Bottino, P., 2014. Thermal behaviour of a series of novel aliphatic bridged polyhedral oligomeric silsesquioxanes (POSSs)/polystyrene (PS) nanocomposites: The influence of the bridge length on the resistance to thermal degradation. Polym. Degrad. Stab. 102, 132–137. https://doi.org/10.1016/j.polymdegradstab.2014.01.029

Blanco, I., Cicala, G., Latteri, A., Saccullo, G., El-Sabbagh, A.M.M., Ziegmann, G., 2017. Thermal characterization of a series of lignin-based polypropylene blends. J. Therm. Anal. Calorim. 127, 147–153. https://doi.org/10.1007/s10973-016-5596-2

Blanco, I., Siracusa, V., 2021. The Use of Thermal Techniques in the Characterization of Bio-Sourced Polymers. Materials 14, 1686. https://doi.org/10.3390/ma14071686

Bogaard, J., Morris, H.R., Whitmore, P.M., 2005. A Method for the Aqueous Deacidification of Oxidized Paper. J. Am. Inst. Conserv. 44, 63–74.

Broda, M., 2020. Natural Compounds for Wood Protection against Fungi—A Review. Molecules 25. https://doi.org/10.3390/molecules25153538

Broda, M., Dąbek, I., Dutkiewicz, A., Dutkiewicz, M., Popescu, C.-M., Mazela, B., Maciejewski, H., 2020. Organosilicons of different molecular size and chemical structure as consolidants for waterlogged archaeological wood – a new reversible and retreatable method. Sci. Rep. 10, 2188. https://doi.org/10.1038/s41598-020-59240-8

Brown, N., Lichtblau, D., Fearn, T., Strlič, M., 2017. Characterisation of 19th and 20th century Chinese paper. Herit. Sci. 5, 47. https://doi.org/10.1186/s40494-017-0158-x

Bugatti, V., Viscusi, G., Naddeo, C., Gorrasi, G., 2017. Nanocomposites Based on PCL and Halloysite Nanotubes Filled with Lysozyme: Effect of Draw Ratio on the Physical Properties and Release Analysis. Nanomaterials 7, 213. https://doi.org/10.3390/nano7080213

Campanella, L., Angeloni, R., Cibin, F., Dell'Aglio, E., Grimaldi, F., Reale, R., Vitali, M., 2021. Capsulated essential oil in gel spheres for the protection of cellulosic cultural heritage. Nat. Prod. Res. 35, 116–123. https://doi.org/10.1080/14786419.2019.1616726

Cavallaro, G., Chiappisi, L., Gradzielski, M., Lazzara, G., 2020a. Effect of the supramolecular interactions on the nanostructure of halloysite/biopolymer hybrids: a comprehensive study by SANS, fluorescence correlation spectroscopy and electric birefringence. Phys. Chem. Chem. Phys. 22, 8193–8202. https://doi.org/10.1039/D0CP01076F

Cavallaro, G., Danilushkina, A.A., Evtugyn, V.G., Lazzara, G., Milioto, S., Parisi, F., Rozhina, E.V., Fakhrullin, R.F., 2017. Halloysite Nanotubes: Controlled Access and Release by Smart Gates. Nanomaterials 7, 199. https://doi.org/10.3390/nano7080199

Cavallaro, G., Lazzara, G., Milioto, S., Parisi, F., 2014. Halloysite nanotubes as sustainable nanofiller for paper consolidation and protection. J. Therm. Anal. Calorim. 117, 1293–1298. https://doi.org/10.1007/s10973-014-3865-5

Cavallaro, G., Milioto, S., Konnova, S., Fakhrullina, G., Akhatova, F., Lazzara, G., Fakhrullin, R., Lvov, Y., 2020b. Halloysite/Keratin Nanocomposite for Human Hair Photoprotection Coating. ACS Appl. Mater. Interfaces 12, 24348–24362. https://doi.org/10.1021/acsami.0c05252

Cavallaro, G., Milioto, S., Lazzara, G., 2020c. Halloysite Nanotubes: Interfacial Properties and Applications in Cultural Heritage. Langmuir 36, 3677–3689. https://doi.org/10.1021/acs.langmuir.0c00573

Cheng, C., Gao, Y., Song, W., Zhao, Q., Zhang, H., Zhang, H., 2020. Halloysite nanotube-based H_2O_2-responsive drug delivery system with a turn on effect on fluorescence for real-time monitoring. Chem. Eng. J. 380, 122474. https://doi.org/10.1016/j.cej.2019.122474

Chivrac, F., Pollet, E., Dole, P., Avérous, L., 2010. Starch-based nano-biocomposites: Plasticizer impact on the montmorillonite exfoliation process. Carbohydr. Polym. 79, 941–947. https://doi.org/10.1016/j.carbpol.2009.10.018

Dang, K.M., Yoksan, R., Pollet, E., Avérous, L., 2020. Morphology and properties of thermoplastic starch blended with biodegradable polyester and filled with halloysite nanoclay. Carbohydr. Polym. 242, 116392. https://doi.org/10.1016/j.carbpol.2020.116392

Dramou, P., Fizir, M., Taleb, A., Itatahine, A., Dahiru, N.S., Mehdi, Y.A., Wei, L., Zhang, J., He, H., 2018. Folic acid-conjugated chitosan oligosaccharide-magnetic halloysite nanotubes as a delivery system for camptothecin. Carbohydr. Polym. 197, 117–127. https://doi.org/10.1016/j.carbpol.2018.05.071

Dresler, C., Saladino, M.L., Demirbag, C., Caponetti, E., Chillura Martino, D.F., Alduina, R., 2017. Development of controlled release systems of biocides for the conservation of cultural heritage. Int. Biodeterior. Biodegrad. 125, 150–156. https://doi.org/10.1016/j.ibiod.2017.09.007

Duce, C., Vecchio Ciprioti, S., Ghezzi, L., Ierardi, V., Tinè, M., 2015. Thermal behavior study of pristine and modified halloysite nanotubes. J. Therm. Anal. Calorim. 121, 1011–1019. https://doi.org/10.1007/s10973-015-4741-7

Dzamukova, M.R., Naumenko, E.A., Lvov, Y.M., Fakhrullin, R.F., 2015. Enzyme-activated intracellular drug delivery with tubule clay nanoformulation. Sci. Rep. 5, 10560.

Fakhrullina, G.I., Akhatova, F.S., Lvov, Y.M., Fakhrullin, R.F., 2015. Toxicity of halloysite clay nanotubes in vivo: a Caenorhabditis elegans study. Environ. Sci. Nano 2, 54–59. https://doi.org/10.1039/C4EN00135D

Fizir, M., Richa, A., He, H., Touil, S., Brada, M., Fizir, L., 2020. A mini review on molecularly imprinted polymer based halloysite nanotubes composites: innovative materials for analytical and environmental applications. Rev. Environ. Sci. Biotechnol. 19, 241–258. https://doi.org/10.1007/s11157-020-09537-x

570 Flint, H.J., Scott, K.P., Duncan, S.H., Louis, P., Forano, E., 2012. Microbial degradation of
571 complex carbohydrates in the gut. Gut Microbes 3, 289–306.
572 https://doi.org/10.4161/gmic.19897
573 Franceschi, E., Palazzi, D., Pedemonte, E., 2001. Thermoanalytical Contribution to the Study on
574 Paper Degradation. Characterisation of Oxidised Paper. J. Therm. Anal. Calorim. 66, 349.
575 https://doi.org/10.1023/A:1012428824378
576 García-Vázquez, R., Rebitski, E.P., Viejo, L., de los Ríos, C., Darder, M., García-Frutos, E.M.,
577 2020. Clay-based hybrids for controlled release of 7-azaindole derivatives as
578 neuroprotective drugs in the treatment of Alzheimer's disease. Appl. Clay Sci. 189, 105541.
579 https://doi.org/10.1016/j.clay.2020.105541
580 Giorgi, R., Bozzi, C., Dei, L., Gabbiani, C., Ninham, B.W., Baglioni, P., 2005. Nanoparticles of
581 Mg(OH)2: Synthesis and Application to Paper Conservation. Langmuir 21, 8495–8501.
582 https://doi.org/10.1021/la050564m
583 Giorgi, R., Dei, L., Ceccato, M., Schettino, C., Baglioni, P., 2002. Nanotechnologies for
584 Conservation of Cultural Heritage: Paper and Canvas Deacidification. Langmuir 18, 8198–
585 8203. https://doi.org/10.1021/la025964d
586 Girardi, F., Bergamonti, L., Isca, C., Predieri, G., Graiff, C., Lottici, P.P., Cappelletto, E., Ataollahi,
587 N., Di Maggio, R., 2017. Chemical–physical characterization of ancient paper with
588 functionalized polyamidoamines (PAAs). Cellulose 24, 1057–1068.
589 https://doi.org/10.1007/s10570-016-1159-8
590 Gorrasi, G., 2015. Dispersion of halloysite loaded with natural antimicrobials into pectins:
591 Characterization and controlled release analysis. Carbohydr. Polym. 127, 47–53.
592 https://doi.org/10.1016/j.carbpol.2015.03.050
593 Gorrasi, G., Pantani, R., Murariu, M., Dubois, P., 2014. PLA/Halloysite Nanocomposite Films:
594 Water Vapor Barrier Properties and Specific Key Characteristics. Macromol. Mater. Eng.
595 299, 104–115. https://doi.org/10.1002/mame.201200424
596 He, B., Lin, Q., Chang, M., Liu, C., Fan, H., Ren, J., 2019. A new and highly efficient conservation
597 treatment for deacidification and strengthening of aging paper by in-situ quaternization.
598 Carbohydr. Polym. 209, 250–257. https://doi.org/10.1016/j.carbpol.2019.01.034
599 Hermawan, A.A., Chang, J.W., Pasbakhsh, P., Hart, F., Talei, A., 2018. Halloysite nanotubes as a
600 fine grained material for heavy metal ions removal in tropical biofiltration systems. Appl.
601 Clay Sci., ACS - SI ICC 2017 XVI International Clay Conference – Clays, from the oceans
602 to space 160, 106–115. https://doi.org/10.1016/j.clay.2017.12.051
603 Isca, C., Di Maggio, R., Pajares Collado, N., Predieri, G., Lottici, P.P., 2019. The use of
604 polyamidoamines for the conservation of iron-gall inked paper. Cellulose 26, 1277–1296.
605 https://doi.org/10.1007/s10570-018-2105-8
606 Jiang, J., Chen, H., Liu, L., Yu, J., Fan, Y., Saito, T., Isogai, A., 2020. Influence of Chemical and
607 Enzymatic TEMPO-Mediated Oxidation on Chemical Structure and Nanofibrillation of
608 Lignocellulose. ACS Sustain. Chem. Eng. 8, 14198–14206.
609 https://doi.org/10.1021/acssuschemeng.0c05291
610 Jiang, Z., Fan, J., Budarin, V.L., Macquarrie, D.J., Gao, Y., Li, T., Hu, C., Clark, J.H., 2018.
611 Mechanistic understanding of salt-assisted autocatalytic hydrolysis of cellulose. Sustain.
612 Energy Fuels 2, 936–940. https://doi.org/10.1039/C8SE00045J
613 Kryuchkova, M., Danilushkina, A., Lvov, Y., Fakhrullin, R., 2016. Evaluation of toxicity of
614 nanoclays and graphene oxide in vivo: a Paramecium caudatum study. Environ. Sci. Nano 3,
615 442–452. https://doi.org/10.1039/C5EN00201J
616 Lazzara, G., Cavallaro, G., Panchal, A., Fakhrullin, R., Stavitskaya, A., Vinokurov, V., Lvov, Y.,
617 2018. An assembly of organic-inorganic composites using halloysite clay nanotubes. Curr.
618 Opin. Colloid Interface Sci. 35, 42–50. https://doi.org/10.1016/j.cocis.2018.01.002
619 Lienardy, A., Damme, P.V., 1990. Practical Deacidification 11, 1–21.
620 https://doi.org/10.1515/rest.1990.11.1.1

Lisuzzo, L., Caruso, M.R., Cavallaro, G., Milioto, S., Lazzara, G., 2021. Hydroxypropyl Cellulose Films Filled with Halloysite Nanotubes/Wax Hybrid Microspheres. Ind. Eng. Chem. Res. 60, 1656–1665. https://doi.org/10.1021/acs.iecr.0c05148
Lisuzzo, L., Cavallaro, G., Milioto, S., Lazzara, G., 2020a. Effects of halloysite content on the thermo-mechanical performances of composite bioplastics. Appl. Clay Sci. 185, 105416. https://doi.org/10.1016/j.clay.2019.105416
Lisuzzo, L., Cavallaro, G., Parisi, F., Milioto, S., Lazzara, G., 2019a. Colloidal stability of halloysite clay nanotubes. Ceram. Int., Thermophysical Aspects of Functional Ceramics and Surfaces 45, 2858–2865. https://doi.org/10.1016/j.ceramint.2018.07.289
Lisuzzo, L., Cavallaro, G., Pasbakhsh, P., Milioto, S., Lazzara, G., 2019b. Why does vacuum drive to the loading of halloysite nanotubes? The key role of water confinement. J. Colloid Interface Sci. 547, 361–369. https://doi.org/10.1016/j.jcis.2019.04.012
Lisuzzo, L., Wicklein, B., Dico, G.L., Lazzara, G., Real, G. del, Aranda, P., Ruiz-Hitzky, E., 2020b. Functional biohybrid materials based on halloysite, sepiolite and cellulose nanofibers for health applications. Dalton Trans. 49, 3830–3840. https://doi.org/10.1039/C9DT03804C
Liu, J., Li, K., Wang, H., Zhu, M., Xu, H., Yan, H., 2004. Self-assembly of hydroxyapatite nanostructures by microwave irradiation. Nanotechnology 16, 82–87. https://doi.org/10.1088/0957-4484/16/1/017
Liu, K., Li, W., Chen, S., Wen, W., Lu, L., Liu, M., Zhou, C., Luo, B., 2020. The design, fabrication and evaluation of 3D printed gHNTs/gMgO whiskers/PLLA composite scaffold with honeycomb microstructure for bone tissue engineering. Compos. Part B Eng. 192, 108001. https://doi.org/10.1016/j.compositesb.2020.108001
Liu, M., Chang, Y., Yang, J., You, Y., He, R., Chen, T., Zhou, C., 2016. Functionalized halloysite nanotube by chitosan grafting for drug delivery of curcumin to achieve enhanced anticancer efficacy. J Mater Chem B 4, 2253–2263. https://doi.org/10.1039/C5TB02725J
Lvov, Y., Wang, W., Zhang, L., Fakhrullin, R., 2016. Halloysite Clay Nanotubes for Loading and Sustained Release of Functional Compounds. Adv. Mater. 28, 1227–1250. https://doi.org/10.1002/adma.201502341
Lvov, Y.M., Shchukin, D.G., Mohwald, H., Price, R.R., 2008. Halloysite Clay Nanotubes for Controlled Release of Protective Agents. ACS Nano 2, 814–820. https://doi.org/doi: 10.1021/nn800259q
M., W.P., Bogaard John, 2009. Determination of the Cellulose Scission Route in the Hydrolytic and Oxidative Degradation of Paper. Restaurator 15, 26–45. https://doi.org/10.1515/rest.1994.15.1.26
Makaremi, M., De Silva, R.T., Pasbakhsh, P., 2015. Electrospun Nanofibrous Membranes of Polyacrylonitrile/Halloysite with Superior Water Filtration Ability. J. Phys. Chem. C 119, 7949–7958. https://doi.org/10.1021/acs.jpcc.5b00662
Marini, F., Tomassetti, M., Vecchio, S., 2012. Detailed kinetic and chemometric study of the cellulose thermal breakdown in artificially aged and non aged commercial paper. Different methods for computing activation energy as an assessment model in archaeometric applications. Chem. Cent. J. 6, S7. https://doi.org/10.1186/1752-153X-6-S2-S7
Meng, B., Mueller, U., Garcia, O., Malaga, K., 2014. Performance of a New Anti-Graffiti Agent Used for Immovable Cultural Heritage Objects. Int. J. Archit. Herit. 8, 820–834. https://doi.org/10.1080/15583058.2012.747116
Motelica, L., Popescu, A., Răzvan, A.-G., Oprea, O., Truşcă, R.-D., Vasile, B.-S., Dumitru, F., Holban, A.-M., 2020. Facile Use of ZnO Nanopowders to Protect Old Manual Paper Documents. Materials 13, 5452. https://doi.org/10.3390/ma13235452
Nunes, C., Coimbra, M.A., Ferreira, P., 2018. Tailoring Functional Chitosan-Based Composites for Food Applications. Chem. Rec. 18, 1138–1149. https://doi.org/10.1002/tcr.201700112
Oh, S.Y., Yoo, D.I., Shin, Y., Kim, H.C., Kim, H.Y., Chung, Y.S., Park, W.H., Youk, J.H., 2005. Crystalline structure analysis of cellulose treated with sodium hydroxide and carbon dioxide

by means of X-ray diffraction and FTIR spectroscopy. Carbohydr. Res. 340, 2376–2391. https://doi.org/10.1016/j.carres.2005.08.007
Okahashi, K., Takeuchi, M., Zhou, Y., Ono, Y., Fujisawa, S., Saito, T., Isogai, A., 2021. Nanocellulose-containing cellulose ether composite films prepared from aqueous mixtures by casting and drying method. Cellulose. https://doi.org/10.1007/s10570-021-03897-5
Owoseni, O., Nyankson, E., Zhang, Y., Adams, S.J., He, J., McPherson, G.L., Bose, A., Gupta, R.B., John, V.T., 2014. Release of Surfactant Cargo from Interfacially-Active Halloysite Clay Nanotubes for Oil Spill Remediation. Langmuir 30, 13533–13541. https://doi.org/10.1021/la503687b
Pasbakhsh, P., Churchman, G.J., Keeling, J.L., 2013. Characterisation of properties of various halloysites relevant to their use as nanotubes and microfibre fillers. Appl. Clay Sci. 74, 47–57. https://doi.org/10.1016/j.clay.2012.06.014
Poggi, G., Giorgi, R., Toccafondi, N., Katzur, V., Baglioni, P., 2010. Hydroxide Nanoparticles for Deacidification and Concomitant Inhibition of Iron-Gall Ink Corrosion of Paper. Langmuir 26, 19084–19090. https://doi.org/10.1021/la1030944
Poggi, G., Sistach, M.C., Marin, E., Garcia, J.F., Giorgi, R., Baglioni, P., 2016. Calcium hydroxide nanoparticles in hydroalcoholic gelatin solutions (GeolNan) for the deacidification and strengthening of papers containing iron gall ink. J. Cult. Herit. 18, 250–257. https://doi.org/10.1016/j.culher.2015.10.005
Poggi, G., Toccafondi, N., Melita, L.N., Knowles, J.C., Bozec, L., Giorgi, R., Baglioni, P., 2014. Calcium hydroxide nanoparticles for the conservation of cultural heritage: new formulations for the deacidification of cellulose-based artifacts. Appl. Phys. A 114, 685–693. https://doi.org/10.1007/s00339-013-8172-7
Rozhina, E., Batasheva, S., Miftakhova, R., Yan, X., Vikulina, A., Volodkin, D., Fakhrullin, R., 2021. Comparative cytotoxicity of kaolinite, halloysite, multiwalled carbon nanotubes and graphene oxide. Appl. Clay Sci. 205, 106041. https://doi.org/10.1016/j.clay.2021.106041
Sadjadi, S., 2020. Halloysite-based hybrids/composites in catalysis. Appl. Clay Sci. 189, 105537. https://doi.org/10.1016/j.clay.2020.105537
Sadjadi, S., Hosseinnejad, T., Malmir, M., Heravi, M.M., 2017. Cu@furfural imine-decorated halloysite as an efficient heterogeneous catalyst for promoting ultrasonic-assisted A3 and KA2 coupling reactions: a combination of experimental and computational study. New J. Chem. 41, 13935–13951. https://doi.org/10.1039/C7NJ02272G
Saladino, M.L., Markowska, M., Carmone, C., Cancemi, P., Alduina, R., Presentato, A., Scaffaro, R., Biały, D., Hasiak, M., Hreniak, D., Wawrzyńska, M., 2020. Graphene Oxide Carboxymethylcellulose Nanocomposite for Dressing Materials. Materials 13, 1980. https://doi.org/10.3390/ma13081980
Schmitz, K., Wagner, S., Reppke, M., Maier, C.L., Windeisen-Holzhauser, E., Benz, J.P., 2019. Preserving cultural heritage: Analyzing the antifungal potential of ionic liquids tested in paper restoration. PLOS ONE 14, e0219650. https://doi.org/10.1371/journal.pone.0219650
Sharma, G., Bala, R., Bala, R., 2017. Digital Color Imaging Handbook. CRC Press. https://doi.org/10.1201/9781420041484
Spepi, A., Duce, C., Pedone, A., Presti, D., Rivera, J.-G., Ierardi, V., Tiné, M.R., 2016. Experimental and DFT Characterization of Halloysite Nanotubes Loaded with Salicylic Acid. J. Phys. Chem. C 120, 26759–26769. https://doi.org/10.1021/acs.jpcc.6b06964
Tarasov, K., Beaunier, P., Che, M., Marceau, E., Li, Y., 2011. Genesis of supported carbon-coated Co nanoparticles with controlled magnetic properties, prepared by decomposition of chelate complexes. J. Nanoparticle Res. 13, 1873–1887. https://doi.org/10.1007/s11051-010-9938-x
Vinokurov, V.A., Stavitskaya, A.V., Chudakov, Y.A., Ivanov, E.V., Shrestha, L.K., Ariga, K., Darrat, Y.A., Lvov, Y.M., 2017. Formation of metal clusters in halloysite clay nanotubes. Sci. Technol. Adv. Mater. 18, 147–151. https://doi.org/10.1080/14686996.2016.1278352

Viseras, M.-T., Aguzzi, C., Cerezo, P., Cultrone, G., Viseras, C., 2009. Supramolecular structure of 5-aminosalycilic acid/halloysite composites. J. Microencapsul. 26, 279–286. https://doi.org/10.1080/02652040802312499

von Klitzing, R., Stehl, D., Pogrzeba, T., Schomäcker, R., Minullina, R., Panchal, A., Konnova, S., Fakhrullin, R., Koetz, J., Möhwald, H., Lvov, Y., 2016. Halloysites Stabilized Emulsions for Hydroformylation of Long Chain Olefins. Adv. Mater. Interfaces 1600435–1600443. https://doi.org/10.1002/admi.201600435

Yamina, A.M., Fizir, M., Itatahine, A., He, H., Dramou, P., 2018. Preparation of multifunctional PEG-graft-Halloysite Nanotubes for Controlled Drug Release, Tumor Cell Targeting, and Bio-imaging. Colloids Surf. B Biointerfaces 170, 322–329. https://doi.org/10.1016/j.colsurfb.2018.06.042

Yang, J., Wu, Y., Shen, Y., Zhou, C., Li, Y.-F., He, R.-R., Liu, M., 2016. Enhanced Therapeutic Efficacy of Doxorubicin for Breast Cancer Using Chitosan Oligosaccharide-Modified Halloysite Nanotubes. ACS Appl. Mater. Interfaces 8, 26578–26590. https://doi.org/10.1021/acsami.6b09074

Yang, X., Zhang, Y., Zheng, D., Yue, J., Liu, M., 2020. Nano-biocomposite films fabricated from cellulose fibers and halloysite nanotubes. Appl. Clay Sci. 190, 105565–105574. https://doi.org/10.1016/j.clay.2020.105565

Yousefi, P., Hamedi, S., Garmaroody, E.R., Koosha, M., 2020. Antibacterial nanobiocomposite based on halloysite nanotubes and extracted xylan from bagasse pith. Int. J. Biol. Macromol. 160, 276–287. https://doi.org/10.1016/j.ijbiomac.2020.05.209

Zhang, H., Cheng, C., Song, H., Bai, L., Cheng, Y., Ba, X., Wu, Y., 2019. A facile one-step grafting of polyphosphonium onto halloysite nanotubes initiated by Ce(IV). Chem. Commun. 55, 1040–1043. https://doi.org/10.1039/C8CC08667B

Zhang, Y., Bai, L., Cheng, C., Zhou, Q., Zhang, Z., Wu, Y., Zhang, H., 2019. A novel surface modification method upon halloysite nanotubes: A desirable cross-linking agent to construct hydrogels. Appl. Clay Sci. 182, 105259–105267. https://doi.org/10.1016/j.clay.2019.105259

Zhao, X., Zhou, C., Liu, M., 2020. Self-assembled structures of halloysite nanotubes: towards the development of high-performance biomedical materials. J Mater Chem B 8, 838–851. https://doi.org/10.1039/C9TB02460C

Zhao, Y., Cavallaro, G., Lvov, Y., 2015. Orientation of charged clay nanotubes in evaporating droplet meniscus. J. Colloid Interface Sci. 440, 68–77. https://doi.org/10.1016/j.jcis.2014.10.050

Zhao, Y., Kong, W., Jin, Z., Fu, Y., Wang, W., Zhang, Y., Liu, J., Zhang, B., 2018. Storing solar energy within Ag-Paraffin@Halloysite microspheres as a novel self-heating catalyst. Appl. Energy 222, 180–188. https://doi.org/10.1016/j.apenergy.2018.04.013